J Appl Electrochem (2009) 39:689–696
DOI 10.1007/s10800-008-9710-4

ORIGINAL PAPER

Understanding the inhibitory effect of sodium oleate on the corrosion of Al and Al–Cu alloys in 1.0 M H_3PO_4 solution—Polarization studies

Mohammed A. Amin

Received: 9 July 2008 / Accepted: 27 October 2008 / Published online: 15 November 2008

Abstract Polarization measurements were employed, as a first step towards studying the corrosion behaviour of Al and two Al–Cu alloys, namely Al–4.5%Cu, and Al–7.5%Cu alloys in deaerated stirred 1.0 M H_3PO_4 solution at 25 °C. Inhibition of Al and Al–Cu alloys corrosion in 1.0 M H_3PO_4 solution, using sodium oleate (SO) as an anionic surfactant inhibitor, was also studied. Polarization curves showed that SO acted as a mixed-type inhibitor to Al corrosion, while it acted mainly as a cathodic inhibitor to the acid corrosion of Al–4.5%Cu, and Al–7.5%Cu alloys. Inhibition is accomplished by inhibitor adsorption on the electrode surface without detectable changes in the chemistry of corrosion. The relationship between surfactant concentration, surfactant critical micellar concentration (CMC), and corrosion inhibition is also discussed based on the Langmuir isotherm assumption, commonly applied in corrosion inhibition evaluations. The protection efficiency increases with increase in surfactant concentration and %Cu in Al samples. Maximum protection efficiency of the surfactant is observed at concentrations around its CMC. The mechanism of adsorption is discussed based on the surface charge of the electrode surface.

Keywords Al · Al–Cu alloys · Corrosion inhibition · Sodium oleate · Phosphoric acid · Polarization

M. A. Amin (✉)
Chemistry Department, Faculty of Science, Ain Shams University, 11566 Abbassia, Cairo, Egypt
e-mail: maaismail@yahoo.com

1 Introduction

Al and its alloys are preferred as materials of construction, because of the light weight of the metal coupled with its strength, good electrical and heat conductivity, and good corrosion resistance. The strength of Al is very much improved when Al is alloyed with Cu. Compared with pure Al, Al–Cu alloys have a lower corrosion resistance [1, 2]. The high corrosion resistance of Al and its alloys is attributed to the formation of a highly protective barrier oxide film which separates the bare metal from the corrosive environment. This passive film on Al and its alloys can be formed directly in humid air or at exposure to an aqueous electrolyte solution. In more acidic or alkaline solutions oxides are rapidly dissolved and general attack results.

Solutions of phosphoric acid are frequently employed for cleaning of Al [3, 4] and in commercial pre-plating anodic oxidation and electro-polishing of Al [5]. In most cases of Al corrosion an additive must be added to the environment in order to modify or hinder corrosion. The protection of Al and its oxide films from corrosion has been studied by many investigators using either inorganic oxidants including chromate [6–9], molybdate [10–12] and tungstate [6, 9], organic compounds having polar groups, such as oxygen, sulphur, and nitrogen [12–17], and heterocyclic compounds containing functional groups and conjugated double bonds [17–20] as inhibitors.

Although surfactants have been widely used, only a few studies have focused on the application of surfactants for corrosion prevention of Al and its alloys [21–23]. In our previous study [24–26], anionic, cationic and non-ionic surfactants were successfully used as corrosion inhibitors for the corrosion of pure Al and some of its alloys in HCl solutions. The main objective here is to investigate the

ability of sodium oleate (SO) as an anionic surfactant to inhibit the corrosion of Al and two Al–Cu alloys in deaerated stirred 1.0 M H_3PO_4 solution under the influence of various experimental conditions using potentiodynamic polarization measurements. It was also the purpose of the present work to apply the Langmuir isotherm assumption to gain more information about the inhibitive effect of the surfactant.

2 Experimental

The working electrodes were made from pure Al (% purity of 99.99) and two Al–Cu alloys, namely Al–4.5%Cu and Al–7.5%Cu alloys. These materials were in the form of sheets, 0.10 cm thick, for surface analysis, and cylindrical rods of base diameter 0.50 cm for electrochemical measurements. Table 1 presents the mass spectroscopic analysis of the two Al–Cu alloys. For electrochemical measurements the cylindrical rods were welded to a Cu-wire for electrical connection and mounted into glass tubes of appropriate diameter using Araldite to offer an active flat disc shaped surface of about 0.20 cm^2 geometric area to contact the test solution. These rods were first briefly ground with no. 600 emery paper, subsequently polished with no. 2000 emery paper, washed with deionized water, degreased with absolute ethanol, dried, and then rapidly rinsed with deionized water, followed by immediate rinsing with absolute ethanol.

A conventional electrochemical cell of capacity 100 mL was used containing three compartments for working, platinum spiral counter and reference electrodes. The reference was a saturated calomel electrode used directly in contact with the working solution. The measurements were carried out in deaerated stirred 1.0 M H_3PO_4 solutions without and with various concentrations (10^{-5}–2×10^{-3} M) of sodium oleate (SO), as an anionic surfactant inhibitor, at 25 °C. All solutions were freshly prepared from analytical grade chemical reagents using doubly distilled water and were used without further purification. For each run a freshly prepared solution as well as a cleaned set of electrodes was used. Each run was carried out in deaerated stirred solutions at the required temperature (±1 °C), using a water thermostat. Electrochemical measurements were performed using a potentiostat/galvanostat (EG&G model 273) and lock-in amplifier (model 5210) connected with a personal computer. Various electrochemical parameters were simultaneously determined using M352 corrosion software from EG&G Princeton Applied Research. The potentiodynamic current–potential curves were carried out at a scan rate of 0.10 mV s^{-1} starting from −1.50 V up to 1.0 V (SCE). Before each polarization experiment the open circuit potential of the working electrode was measured as a function of time during 24 h, the time necessary to reach a quasi-stationary value for the open circuit potential.

Table 1 Mass spectroscopic analysis of the two Al–Cu alloys

Alloy	Al	Cu	Mn	Si	Mg	Zn	Sn	Cr	Ti
Al–4.5%Cu	95.212	4.5	0.02	0.03	0.20	0.022	0.005	0.001	0.01
Al–7.5%Cu	92.212	7.5	0.02	0.03	0.20	0.022	0.005	0.001	0.01

3 Results and discussion

3.1 Potentiodynamic polarization measurements

In Fig. 1, the polarization curves recorded for Al, Al–4.5%Cu and Al–7.5%Cu alloys in deaerated stirred 1.0 M H_3PO_4 solution, are shown. The effect of SO concentration (10^{-5}–2×10^{-3} M), the same concentration range as used in a previous study [27], on the potentiodynamic anodic and cathodic polarization curves of the three Al samples in 1.0 M H_3PO_4 solution was studied at a scan rate of 0.10 mV s^{-1} at 25 °C. Some results are depicted in Fig. 2. Tables 2, 3, 4 present the electrochemical parameters (E_{corr}, j_{corr}, b_c, and R_P) associated with polarization measurements at different SO concentrations for the three samples. Protection efficiency (%P) values were also calculated for the three samples and are included in Tables 2, 3, 4, using Eq. 1:

$$\%P = 100 \times \left[\left(j^{o}_{corr} - (j_{corr})_i\right)/j^{o}_{corr}\right] \quad (1)$$

where $\left(j^{\circ}_{corr}\right)$ and $(j_{corr})_i$ are the corrosion current densities without and with inhibitor. Accurate evaluation of

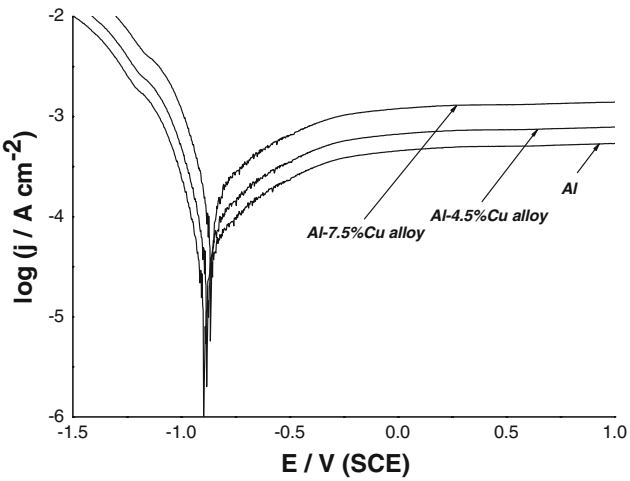

Fig. 1 Polarization curves recorded for Al, Al–4.5%Cu and Al–7.5%Cu alloys in deaerated stirred 1.0 M H_3PO_4 solution at a scan rate of 0.10 mV s^{-1} at 25 °C

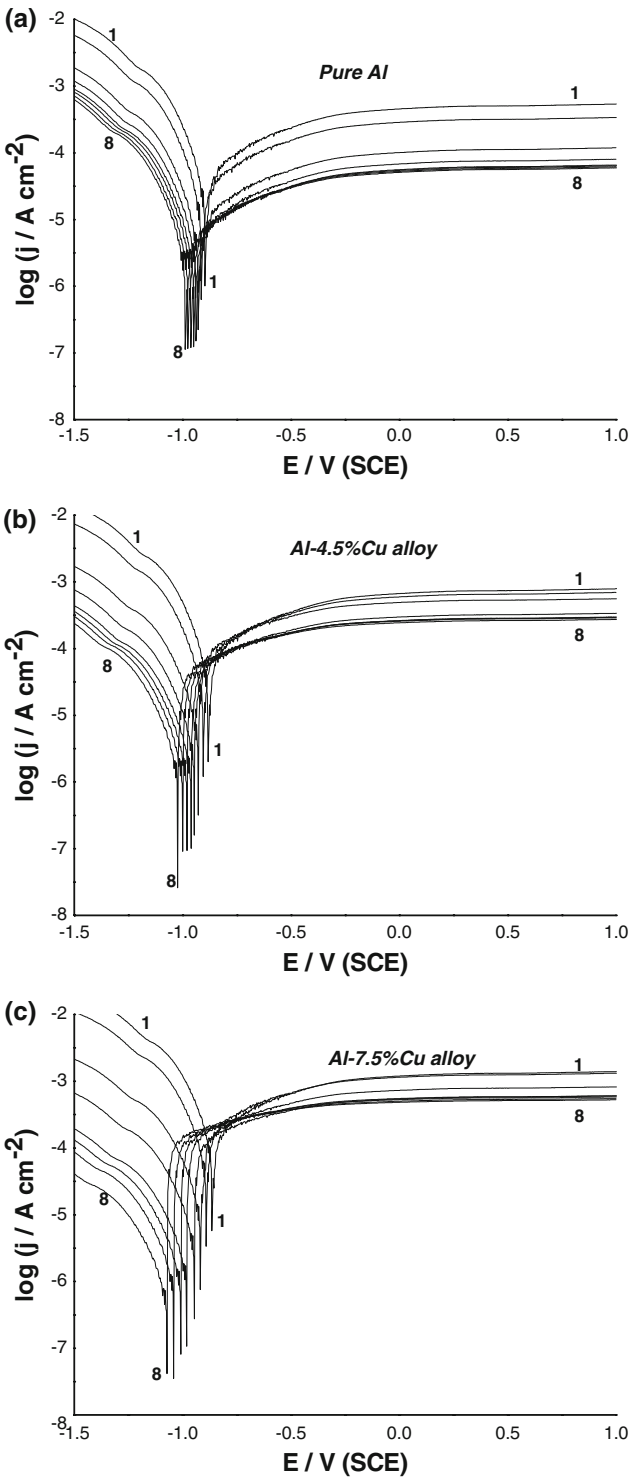

◀ **Fig. 2** Effect of SO concentration on polarization curves of (**a**) Al, (**b**) Al–4.5%Cu alloy, and (**c**) Al–7.5%Cu alloy in deaerated stirred 1.0 M H_3PO_4 solution at a scan rate of 0.10 mV s^{-1} at 25 °C. (1) blank; (2) 8 × 10^{-5} M SO; (3) 25 × 10^{-5} M SO; (4) 75 × 10^{-5} M SO; (5) 125 × 10^{-5} M SO; (6) 150 × 10^{-5} M SO; (7) 175 × 10^{-5} M SO; (8) 200 × 10^{-5} M SO

corrosion rate (i.e., corrosion current density, j_{corr}) from the anodic branches, and therefore the anodic Tafel slope (b_a), is impossible, simply because the experimental anodic polarization curves presented in Figs. 1 and 2 do not exhibit linear Tafel regions. This is because the absence of linearity in the anodic branches prevents linear extrapolation to the corrosion potential, E_{corr}. This was the reason why values of b_a, calculated from the software, were not introduced in Tables 2, 3, 4. However, the cathodic branch, as will be discussed later, is under activation control and exhibits linearity in accord with Tafel relationship. The corrosion rate, and therefore the cathodic Tafel slope (b_c) may be estimated accurately by extrapolating the cathodic linear region back to E_{corr}. It is obvious from Figs. 1 and 2 that no-active passive transition was observed and the current seems to be constant at high anodic potentials. Based on data of Tables 2, 3, 4, in SO free-H_3PO_4 solutions, the corrosion current densities, j_{corr}, of Al, Al–4.5%Cu and Al–7.5%Cu alloys were estimated to be 5.0 × 10^{-2}, 7.5 × 10^{-2} and 17.8 × 10^{-2} mA cm^{-2}, respectively. Similar results were previously obtained during corrosion of Al, Al–6061 and Al–4.8%Cu alloys in borate and chloride solutions of different pH after long immersion times [28]. These results indicate that Al–Cu alloys, under these conditions, are less corrosion resistant than pure Al, and the corrosion resistance decreases with increase in %Cu in the Al samples. It seems therefore that alloying Al with Cu, decreases the corrosion resistance after prolonged immersion in H_3PO_4 solutions to an extent depending on the Cu percentage in Al [29]. This is also reflected in the polarization curve (Fig. 1) in which the passive current, j_{pass}, is enhanced upon alloying Al with Cu. This behaviour, as previously reported by Badawy et al. [28], can be attributed to the effect of the alloying element. Based on XPS and SEM examinations of the electrode surface, Badawy and Al-Kharafi [28] demonstrated that the presence of Cu on the Al–Cu surface is responsible for the higher rates of corrosion recorded for Al–Cu alloys. Alloyed Cu, as previously reported [28], initiates cathodic areas on the alloy surface (or flawed regions in the barrier film) which leads to the observed decrease in the corrosion resistance of the alloy after long immersion in the test solution (here the immersion time is 24 h; see details in the experimental part).

Figure 2 shows, for all cases, that the addition of SO enhances both anodic and cathodic overpotentials. These results indicate that the presence of SO inhibits both anodic and cathodic processes. However, upon alloying Al with Cu (Figs. 2b, c), the cathodic overvoltage is much greater than the anodic one. In this case the rate of cathodic reaction controls the rate of corrosion. At the same time, the corrosion potential (E_{corr}) values, in all cases, are displaced negatively. This negative shift in E_{corr} depends on

Table 2 The electrochemical parameters ($j_{corr.}$, $E_{corr.}$, b_c and R_p) associated with polarization measurements of Al in deaerated stirred 1.0 M H_3PO_4 solution in the absence and presence of different concentrations of SO at 25 °C

$C_{inhib.} \times 10^5$/M	$(j_{corr} \times 10^2)$/ mA cm^{-2}	E_{corr}/V(SCE)	b_c/V $dec.^{-1}$	$(R_p \times 10^{-2})$/ Ω cm^2	%P
Blank	5.00	−0.897	−0.154	4.95	–
1	4.70	−0.902	−0.153	5.27	6.00
2	4.40	−0.908	−0.152	5.62	12.00
5	3.84	−0.911	−0.153	6.44	23.20
8	3.15	−0.914	−0.154	7.86	37.00
10	2.90	−0.920	−0.156	8.53	42.00
25	1.11	−0.928	−0.157	22.20	77.80
50	0.91	−0.932	−0.156	27.29	81.80
75	0.75	−0.937	−0.155	33.22	85.00
100	0.64	−0.942	−0.155	38.61	87.20
125	0.61	−0.948	−0.153	40.84	87.80
150 (CMC)	0.60	−0.961	−0.152	41.63	88.00
175	0.58	−0.975	−0.153	42.38	88.40
200	0.56	−0.988	−0.154	43.92	88.80

Table 3 The electrochemical parameters ($j_{corr.}$, $E_{corr.}$, b_c and R_p) associated with polarization measurements of Al–4.5%Cu alloy in deaerated stirred 1.0 M H_3PO_4 solution in the absence and presence of different concentrations of SO at 25 °C

$C_{inhib.} \times 10^5$/M	$(j_{corr} \times 10^2)$/ mA cm^{-2}	E_{corr}/V(SCE)	b_c/V $dec.^{-1}$	$(R_p \times 10^{-2})$/ Ω cm^2	%P
Blank	7.50	−0.882	−0153	3.70	–
1	7.00	−0.888	−0.152	3.96	6.67
2	6.53	−0.895	−0.151	4.25	12.93
5	5.63	−0.900	−0.152	4.93	24.93
8	4.50	−0.904	−0.153	6.17	40.00
10	4.10	−0.920	−0.155	6.77	45.33
25	1.20	−0.927	−0.154	23.13	84.00
50	0.86	−0.935	−0.153	32.17	88.53
75	0.60	−0.946	−0.152	46.25	92.00
100	0.43	−0.955	−0.154	64.35	94.27
125	0.38	−0.960	−0.151	74.00	94.93
150 (CMC)	0.35	−0.980	−0.153	77.89	95.33
175	0.34	−0.999	−0.152	81.86	95.47
200	0.33	−1.021	−0.152	90.69	95.60

sample composition. It enhances with increase in percentage alloyed Cu (see Figs. 2a–c, as well as values of E_{corr} presented in Tables 2, 3, 4). This means that the cathodic process is highly suppressed by the surfactant addition upon alloying Al with Cu. Thus SO behaves as a mixed-type inhibitor to Al corrosion, while it acts mainly as a cathodic inhibitor to the corrosion of the two tested Al–Cu alloys, by retarding hydrogen evolution on cathodic sites (alloyed Cu-atoms) of the electrode surface.

The cathodic inhibitive action of SO may be interpreted on the basis that the potential at the cathodic sites (Cu-atoms) is more positive than that at the anodic sites (Al-atoms) and therefore the electrostatic adsorption of the anionic surfactant, as will be discussed later, is more likely at the cathodic sites. In other words, preferential adsorption of the anionic surfactant occurs on the cathodic sites, namely Cu-atoms, resulting in a marked increase in the cathodic overpotential.

The shapes of the polarization plots for inhibited electrodes are not substantially different from those of uninhibited electrodes. The presence of surfactant decreases the corrosion rate but does not change other aspects of the behaviour. This means that the inhibitor does not alter the electrochemical reactions responsible for corrosion. In all cases it is observed that the hydrogen evolution reaction is activation controlled since the cathodic portions rise to Tafel lines. It is clear that the mechanism of proton reduction is not modified upon surfactant addition. This is clearly seen from the low variation in the cathodic Tafel slope (b_c), Tables 2, 3, 4.

Table 4 The electrochemical parameters ($j_{corr.}$, $E_{corr.}$, b_c and R_p) associated with polarization measurements of Al–7.5%Cu alloy in deaerated stirred 1.0 M H_3PO_4 solution in the absence and presence of different concentrations of SO at 25 °C

$C_{inhib.} \times 10^5$/M	$(j_{corr} \times 10^2)$/ mA cm^{-2}	E_{corr}/V(SCE)	b_c/V dec^{-1}	$(R_p \times 10^{-2})$/ Ω cm^2	%P
Blank	17.8	−0.866	−0.150	1.55	–
1	16.60	−0.875	−0.151	1.66	6.74
2	15.42	−0.882	−0.150	1.79	13.37
5	13.19	−0.887	−0.149	2.09	25.90
8	10.43	−0.891	−0.151	2.65	41.40
10	9.45	−0.910	−0.152	2.92	46.91
25	2.33	−0.917	−0.151	11.87	86.91
50	1.50	−0.938	−0.150	18.45	91.57
75	0.85	−0.945	−0.151	32.43	95.22
100	0.44	−0.965	−0.153	63.27	97.53
125	0.30	−0.980	−0.150	92.81	98.31
150 (CMC)	0.25	−1.008	−0.151	109.15	98.60
175	0.21	−1.040	−0.149	131.36	98.82
200	0.13	−1.070	−0.150	215.28	99.28

The absence of significant changes in the cathodic Tafel slope in the presence of inhibitor indicates that the hydrogen evolution is slowed by the surface blocking effect of the inhibitor. The inhibitive action of SO, therefore may be related to adsorption and formation of a barrier film on the electrode surface. EDX examinations of the surface for the three Al samples under various experimental conditions confirmed the existence of an adsorbed film of inhibitor. EDX examinations, together with impedance studies, will be included in further work.

Tables 2, 3, 4 show that the values of (%P) for the three samples, at a given inhibitor concentration, decrease in the order: (Al–7.5%Cu) > (Al–4.5%Cu) > Al. This trend may be explained on the basis that as the Cu content is increased, Cu atoms will appear with greater frequency at the alloy surface due to preferential dissolution of Al, and therefore the number of cathodic sites increases. Since the adsorption of the anionic surfactant is more likely at the cathodic sites (Cu-atoms), as previously mentioned, more anionic surfactant molecules are adsorbed on these sites. This means that the large number of cathodic sites, constituted by alloyed Cu-atoms, require a high concentration of SO to be blocked. This condition allows suppression of the hydrogen evolution reaction, corresponding to a marked decrease in the corrosion rate. Consequently, in SO-H_3PO_4 containing solutions, the corrosion rate of Al decreases when alloyed with Cu at concentrations of inhibitor close to its CMC (Tables 2, 3, 4).

Thus alloyed Cu-atoms tend to become preferential cathodic sites for the electrostatic adsorption of the anionic surfactant. However, this point is not fully clear, and more research is needed to clarify the role played by alloyed Cu-atoms in enhancing electrostatic surfactant adsorption. In all cases, the corrosion current density, j_{corr}, decreases with increase in SO concentration. Higher inhibition efficiencies are observed when the concentration of the surfactant reaches values close to its CMC, 1.5×10^{-3} M [30].

The critical micellar concentration (CMC) is a key indicator in determining the effectiveness of surfactants as corrosion inhibitors [31, 32]. Above the CMC, increasing surfactant concentration leads to the gradual formation of multilayers that further reduce the rate of corrosion beyond what can be achieved with monolayer coverage below the CMC. However, concentration changes above the CMC lead to smaller changes in inhibition (see data in Tables 2, 3, 4 at $C_{SO} >$ CMC) since the changes above the CMC result only in additional coverage beyond the monolayer level, which is already sufficient for significant inhibition. In contrast, at surfactant concentration levels well below the CMC, inhibition increases rapidly with increasing surfactant concentration, because the surface is filling with adsorbed surfactant molecules from low coverage to monolayer coverage. Therefore, an excellent surfactant inhibitor is one that aggregates or adsorbs at low concentrations. In other words, surfactants with low CMC values are desirable, because they adsorb at low concentrations. Above all, the critical micellar concentration (CMC) is an important parameter to predict surfactant performance as a corrosion inhibitor. As indicated by the Langmuir isotherm assumption [23, 33–36], the rate of corrosion is proportional to surface sites that are not occupied by surfactant molecules. This leads to:

$$j_{corr}^{-1} = k_1 + k_2 C_{surfactant} \quad (2)$$

where k_1 is a constant representing the baseline j_{corr}^{-1} without any surfactant inhibitor, k_2 is related to the ability of surfactant to adsorb, and $C_{surfactant}$ obviously represents surfactant concentration. Thus, if the Langmuir model is

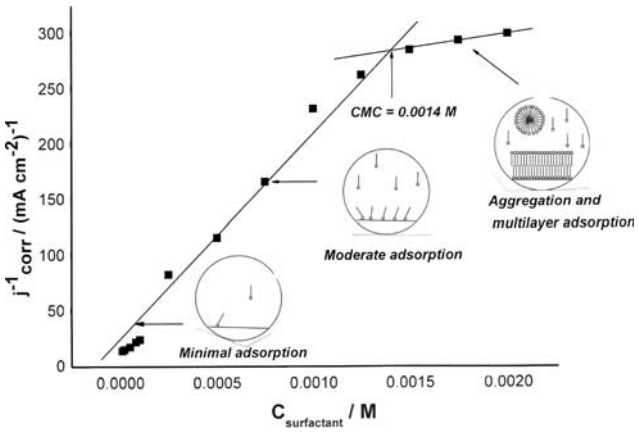

Fig. 3 Dependence of the reciprocal of the corrosion current density, j^{-1}_{corr}, on surfactant concentration, $C_{surfactant}$, for the Al–4.5%Cu alloy samples in deaerated stirred 1.0 M H_3PO_4 solution at 25 °C. Different modes of adsorption presented in the insert were taken from [35]

obeyed a plot of j^{-1}_{corr} versus surfactant concentration should yield a linear relationship as shown in Fig. 3. A linear trend below the CMC with a large slope and another trend with some linearity above the CMC with a reduced slope were obtained. The CMC value calculated from this plot is very close to that previously calculated [27, 30]. The change in slope above the CMC is indicative of the transition from traditional submonolayer-level Langmuir adsorption to multilayer adsorption. It is likely that additional surface coverage in the form of multi-layers and an associated increase in surface and boundary layer viscosity that result at surfactant concentrations above the CMC are responsible for the increase in j^{-1}_{corr} values above the CMC (see linearity with the reduced slope beyond CMC).

This trend can be explained from the work of Free [32]. He reported that, at a coverage of one monolayer or less, surfactant molecules can inhibit either the cathodic or anodic reaction by occupying reactive sites, or by simply providing resistance to the supply of oxidant or the transport of reaction products. Once the surface is filled with surfactant molecules and additional molecules form multiple layer structures, the added surfactant molecules no longer have direct access to the surface. Consequently, the additional molecules that adsorb at concentrations above the CMC must inhibit corrosion by offering additional resistance to the transport of necessary elements rather than by occupying reactive sites directly. Increased corrosion inhibition by surfactant molecules above the CMC due to increased resistance for necessary molecular transport is generally supported by a variety of data [37–39].

3.2 Surface charge of the electrode surface

It is well known that terminal oxygen atoms at metal oxide surfaces react with water, forming hydroxylated sites, or hydroxide layers at the surface (M–OH), that impart a pH-dependent surface charge. The polar hydroxyl ($-OH^-$) groups may cause the surface to attract and physically adsorb a single or several additional layers of polar water molecules. An oxide or hydroxide surface (M–OH) can become charged by reacting with H^+ or OH^- ions due to surface amphoteric reactions, Eqs. 3 and 4. At low pH, a hydroxide surface adsorbs protons to produce positively charged surfaces ($M–OH_2^+$). At high pH they lose protons to produce negatively charged surfaces ($M–O^-$).

$$M-OH + H^+ \leftrightarrow M-OH_2^+ \quad (3)$$

$$M-OH + OH^- \leftrightarrow M-O^- + H_2O \quad (4)$$

The number of these sites and the surface charge of the oxide are determined by the pH of the solution. Surface charge influences adsorption of ions from solution and other interfacial phenomena [40, 41]. The pH of the potential of zero charge (PZC) for aluminium oxides/hydroxides is between 6 and 9, and in acidic solution, the accumulation of $Al–OH_2^+$ species accounts for the surface charge [42, 43]. In acidic solution, therefore the positively charged surface sites will electrostatically attract anions present in solution, and repel cations.

3.3 Mechanism of inhibition and mode of SO adsorption

Adsorption of surfactants on corroding metal surfaces depends mainly on the charge of the metal surface, the charge or the dipole moment of surfactants, and the adsorption of other ionic species if it is electrostatic in nature [44].

SO in solution will ionize out negatively charged alkyl acid radicals, namely oleate anions, which can easily be adsorbed by the Al surface with the hydrophilic group facing the electrode surface and the hydrophobic group facing the liquid medium. This phenomenon is more likely to take place when the concentration of the surfactants is near the CMC. The inhibitive action of SO in H_3PO_4 solution, therefore, results from physical (electrostatic) adsorption of the negatively charged oleate anions to the positively charged electrode surface, forming a barrier. In the early stages of adsorption (low surface coverage), i.e., at low SO concentrations, the adsorption of the hydrocarbon chain (due to the presence of the "–CH=CH–" group) and the electrostatic adsorption of the oleate anions (via the carboxylate group) on the positively charged electrode surface take place simultaneously. This model suggests that the adsorbed oleate anions cover a large area, thereby inhibiting corrosion effectively. This may be the reason why the protection efficiency increases markedly with $C_{surfactant}$ below CMC, Tables 2, 3, 4.

When the concentration of SO increases, more oleate anions electrostatically adsorb on the electrode surface. In this case, the physi-sorption of the hydrocarbon chain may be ignored. A hemimicelle barrier composed of oleate anions will form over the whole surface due to the interaction between hydrocarbon chains via van der Waals forces. The barrier becomes more compact and protective with adsorption of more oleate anions. Thus the inhibition efficiency of SO increases with increase in its concentration.

There is also a possibility that some SO transforms into the corresponding acid, namely oleaic acid (OA), in phosphoric acid solution. Thus, an equilibrium exists between SO and OA. It is probable that OA exists in solution in the form of colloid precipitate due to its quite low solubility. Colloidal precipitates of this acid are charged positively [45, 46] when the pH is below 3. Since the electrode surface is charged positively, it is impossible for the colloidal particles to adsorb on the surface directly through electrostatic attraction.

The positive colloidal particles of the acid (SO) may electrostatically adsorb on the electrode surface covered with an adsorbed negative layer of oleate anions. It is probable that after these molecules are adsorbed on the Al surface by electrostatic forces, they may still react with Al to form chemical bonds. Chemisorption of SO will be fully discussed in a separate study of the temperature effect. As the monomolecular adsorption layer effectively isolates the aluminum from contact with the medium, H^+ ions can hardly penetrate the dense hydrophobic group. Thus the energy barrier of the corrosion reaction is greatly increased.

4 Conclusion

The influence of sodium oleate (SO), as an anionic surfactant inhibitor, on the corrosion behaviour of Al, Al–4.5%Cu and Al–7.5%Cu alloys in deaerated stirred 1.0 M H_3PO_4 solution was investigated using polarization studies. The principal results can be summarised as follows.

Polarization methods showed that in SO-free H_3PO_4 solutions, the rate of corrosion of the three tested Al samples increases in the order: Al < Al–4.5%Cu < Al–7.5%Cu. This sequence is reversed in SO-H_3PO_4 containing solutions, where the presence of alloyed Cu enhanced the electrostatic adsorption of oleate anions on the electrode surface. Polarization measurements show that SO functions as a mixed-type inhibitor to Al corrosion, while it acts predominantly as a cathodic inhibitor for the two Al–Cu alloys. The surfactant adsorbs on the electrode surface without modifying the mechanism of hydrogen evolution reaction. The cathodic process is activation controlled even in the presence of SO. The inhibition efficiency of SO increases with increase in its concentration. Maximum protection efficiencies were obtained at SO concentrations close to its CMC.

References

1. Nakazato RZ, Codaro EN, Ribeiro LMF, Hein LRO (2001) Prakt Metall 38:301
2. Sharma AK, Kumar CS, Mayanna SN, Mahendra KN, Rani RU (1999) Appl Surf 151:280
3. Champion FA (1964) Corrosion testing procedures. Wiley, NY, p 188
4. Godard HP, Jepson WB, Bothwell MR, Kane RL (1967) The corrosion of light metals. Wiley, NY, p 52
5. Fontana MG, Staehle RW (eds) (1970) Advances in corrosion science and technology, vol 1. Plenum, NY, p 248
6. Abd El Rehim SS, Hassan HH, Amin MA (2002) Appl Surf Sci 187:279
7. Badawy WA, Al-Kharafi FM, El-Azab AA (1999) Corros Sci 41:709k
8. Brett CMA, Gomes IAR, Martins JPS (1994) Corros Sci 36:915
9. Zein El Abedin S (2001) J Appl Electrochem 31:711
10. Natishan PM, McCafferty E, Hubler GK (1988) J Electrochem Soc 135:321
11. Emregul KC, Aksut AA (2003) Corros Sci 45:2415
12. Sherif EM, Park S-M (2005) J Electrochem Soc 152:B205
13. Ogurtsov NA, Pud AA, Kamarchik P, Shapoval GS (2004) Synth Met 143:43
14. Zhu D, van Ooij WJ (2003) Corros Sci 45:2163
15. Zhu D, van Ooij WJ (2003) Corros Sci 45:2177
16. Doulami S, Beligiannis K, Dimogerontakis TH, Ninni V, Tsangaraki-Kaplanoglou I (2004) Corros Sci 46:1765
17. Ebenso EE (2002) Mater Chem Phys 7:62
18. Ferreria ES, Giacomelli C, Giacomelli FC, Spinelli A (2004) Mater Chem Phys 83:129
19. Saidman SB, Bessone JB (2002) J Electroanal Chem 521:87
20. Riggs OL Jr (1973) Corrosion inhibitors, 2nd edn. C C Nathan, Houston
21. Branzoi V, Golgovici F, Branzoi F (2002) Mater Chem Phys 78:122
22. Osman MM (2001) Mater Chem Phys 71:12
23. Zhao T, Mu G (1999) Corros Sci 41:1937
24. Abd El Rehim SS, Hassan HH, Amin MA (2001) Mater Chem Phys 70:64
25. Abd El Rehim SS, Hassan HH, Amin MA (2002) Mater Chem Phys 78:33
26. Abd El Rehim SS, Hassan HH, Amin MA (2004) Corros Sci 46:5
27. Amin MA (2006) J Appl Electrochem 36:215
28. Badawy WA, Al-Kharafi FM (1997) Corros Sci 39:681
29. Hollingworth EH, Hunsicker HY (1990) Corrosion resistance of aluminium alloys in metals handbook. 9th ed. OH, USA: American Society for Metals, Metals Park. 2: 204236
30. Tarasova NS, Khachaturyan MA, Nikolaev LA (1984) Russ J Phys Chem 58:628
31. Rozenfeld IL (1981) Corrosion inhibitors. McGraw-Hill, New York, p 97
32. Free ML (2004) Corros Sci 46:2601
33. Langmuir I (1947) J Am Chem Soc 39:848
34. EI-Awady AA, Abd-EI-Nabey BA, Aziz SG (1992) J Electrochem Soc 139:2
35. Free ML (2002) Corros Sci 44:2865
36. Omanovic S, Roscoe SG (2000) Corrosion 56:684

37. Luo H, Guan YC, Han KN (1998) Corrosion 54:726
38. Bregmann JI (1963) Corrosion inhibitors. MacMillan, New York
39. Aramaki K, Hackerman N (1969) J Electrochem Soc 116:568
40. Benerje G, Malhotra SN (1992) Corrosion 48:10
41. Brown GE (1999) Chem Rev 99:77
42. Hohl H, Stumm M (1976) J Colloid Int Sci 55:281
43. Wood R, Fornasiero D, Ralston J (1990) Colloids Surf 51:389
44. Luo H, Guan YC, Han KN (1998) Corrosion 54:619
45. Vermilyea DA (1972) 1st International congress metal corrosion. Butterworths, London, p 62
46. Miller CA, Qutubuddin S (1987) In: Eike H-F, Parfitt CD (eds) Surfactant science series, vol 21. Marcel Dekker, Inc, New York, p 166